3712 *Chem. Mater.* **2010,** *22,* 3712–3724
DOI:10.1021/cm100674p

CHEMISTRY OF MATERIALS
Article

# Thermoresponsive Amphiphilic Diblock Copolymers Synthesized by MADIX/RAFT: Properties in Aqueous Solutions and Use for the Preparation and Stabilization of Gold Nanoparticles

Stéphanie Sistach,[†,‡] Mariana Beija,[†,‡] Virginie Rahal,[†,‡] Annie Brûlet,[#] Jean-Daniel Marty,*[,†,‡] Mathias Destarac,*[,§,⊥] and Christophe Mingotaud[†,‡]

[†]*Université de Toulouse, UPS, IMRCP, 118 route de Narbonne, F-31062 Toulouse, France,* [‡]*CNRS, IMRCP, UMR 5623, F-31062 Toulouse, France,* [§]*Université de Toulouse, UPS, LHFA, 118 route de Narbonne, F-31062 Toulouse, France,* [⊥]*CNRS, LHFA UMR 5069, F-31062 Toulouse, France, and* [#]*Laboratoire Léon Brillouin, UMR12 CEA-CNRS, CEA Saclay, F-91191 GIF/Yvette, France*

*Received March 5, 2010. Revised Manuscript Received April 28, 2010*

Well-defined diblock copolymers comprising thermosensitive poly(*N*-isopropyl acrylamide) (PNIPAM) and poly(*n*-butylacrylate) (PBA) blocks were synthesized by macromolecular design by interchange of xanthates (MADIX)/reversible addition−fragmentation chain transfer polymerization (RAFT) using a xanthate-type mediating agent. Their behavior in aqueous solution as a function of temperature was studied by scattering and microscopy techniques. The cloud point temperature values were strongly correlated to the hydrophobic content of the copolymers. Moreover, above the cloud point, the block copolymer structure led to the formation of large reversible aggregates with well-defined sizes. Those polymers were then used to study the synthesis and stability of gold nanoparticles (AuNPs) dispersions either by coating preformed AuNPs or by in situ preparation. In this latter case, we showed that the appropriate choice of polymer concentration allows one to control the size of the AuNPs. Furthermore, the AuNPs were embedded within globules of diblock copolymers, this type of architecture providing long-term stability as well as a thermosensitivity to the AuNPs.

## 1. Introduction

Macromolecular engineering by controlled radical polymerization (CRP) offers an infinite array of complex polymer architectures with predetermined molecular weights, molecular weight distributions, compositions, and functionalities.[1] Particular attention was paid to designing smart copolymers that dramatically change their properties by responding to a variety of external stimuli like temperature, pH, light, electric field, chemicals, and ionic strength.[2] Among them, thermosensitive block copolymers were widely investigated for their property to reversibly self-assemble in water, leading to aggregate morphologies like micelles or vesicles of particular interest for emulsification, dispersion, encapsulation, and active delivery purposes. The easiness of access to tailor-made polymers by CRP is strongly dependent on the choice of the polymerization technology. Macromolecular design by interchange of xanthates (MADIX)[3]/reversible addition−fragmentation chain transfer polymerization (RAFT)[4] technologies are undoubtedly the most facile method for preparing controlled polymer architectures in water or polar organic solvents with the possibility of including a multitude of functional groups (e.g., −OH, −COOH, $-SO_3H$, $-NR_2$, cationic, zwitterionic groups, etc.) without resorting to tedious protection chemistry.[5] Another major advantage of MADIX/RAFT is its exceptional ability to control the polymerization of acrylamido monomers in contrast to other main CRP processes.[6] This opens access to numerous well-defined copolymers with acrylamido-based blocks exhibiting a lower critical solution temperature (LCST).[7]

Over the years, the MADIX/RAFT process showed its great potential for designing hydrophilic−hydrophobic and double hydrophilic (DHBC) diblock copolymers.[3] In particular, many studies were dedicated to the synthesis[6,8]

*Corresponding author. E-mail: marty@chimie.ups-tlse.fr (J.-D.M.); destarac@chimie.ups-tlse.fr (M.D.).

(1) Matyjaszewski, K.; Gnanou, Y.; Leibler, L. *Macromolecular Engineering: Precise Synthesis, Materials Properties, Applications*; Wiley: New York, 2007; Vol. *1*.
(2) (a) Liu, F.; Urban, M. W. *Prog. Polym. Sci.* **2010**, *35*(1−2), 3–23. (b) Stuart, M. A. C.; Huck, W. T. S.; Genzer, J.; Müller, M.; Ober, C.; Stamm, M.; Sukhorukov, G. B.; Szleifer, I.; Tsukruk, V. V.; Urban, M.; Winnik, F.; Zauscher, S.; Luzinov, I.; Minko, S. *Nat. Mater.* **2010**, *9*(2), 101−113.
(3) Taton, D.; Destarac, M.; Zard, S. Z. Macromolecular Design by Interchange of Xanthates: background, design, scope and applications. In *Handbook of RAFT Polymerization*; Barner-Kowollik, C., Ed.; Wiley−VCH: Weinheim, Germany, 2008; p 373.
(4) Barner-Kowollik, C., In *Handbook of RAFT Polymerization*, Barner-Kowollik, C., Ed.; Wiley−VCH: Weinheim, Germany, 2008.
(5) Boyer, C.; Bulmus, V.; Davis, T. P.; Ladmiral, V.; Liu, J.; Perrier, S. b. *Chem. Rev.* **2009**, *109*(11), 5402–5436.
(6) (a) Taton, D.; Wilczewska, A. Z.; Destarac, M. *Macromol. Rapid Commun.* **2001**, *22*(18), 1497–1503. (b) Lowe, A. B.; McCormick, C. L. *Prog. Polym. Sci.* **2007**, *32*(3), 283–351.
(7) McCormick, C. L.; Sumerlin, B. S.; Lokitz, B. S.; Stempka, J. E. *Soft Matter* **2008**, *4*(9), 1760–1773.
(8) Jacquin, M.; Muller, P.; Talingting-Pabalan, R.; Cottet, H.; Berret, J. F.; Futterer, T.; Theodoly, O. J. *Colloid Interface Sci.* **2007**, *316*(2), 897–911.

 Published on Web 05/25/2010 

and the physicochemical properties of block copolymers comprising a weak polyelectrolyte block, e.g., poly(acrylic acid) (PAA).[9] For instance, anionic-neutral DHBCs comprising a PAA block and a polyacrylamide (PAm) block were efficiently converted into hybrid polyion complex micelles in the presence of positively charged polymers, surfactants, or metal ions. The micellar structures were used as efficient nanoreactors for polymer-templated mineral nanoparticle synthesis.[10] Another strategy for obtaining polymer−mineral hybrid nanomaterials was to control the association of preformed rare earth nanoparticles via the PAA block whereas the PAm played the role of steric barrier against particle aggregation.[11]

The evaluation of the self-assembling properties in water of PAA-based amphiphilic diblock copolymers revealed marked differences in behaviors depending on the nature of the hydrophobic block. Indeed, the micellar structures evolved from frozen colloids in the case of polystyrene cores to true macromolecular surfactants in the case of poly(diethyleneglycol acrylate) (PDEGA).[12] An intermediate behavior was obtained in the case of the soft poly(*n*-butyl acrylate) (PBA) hydrophobic block, for which micellar aggregates with slow adsorption properties were characterized. The interesting interfacial properties of such amphiphilic diblock copolymers were promoted toward the dispersion and stabilization of pigments and most importantly in the field of emulsion stabilization. For instance, the molecular weight and hydrophobic−hydrophilic balance of the block copolymers were finely tuned in order to stabilize or costabilize either direct or inverse emulsions for various applications.[13]

Recently, the MADIX/RAFT process was successfully implemented to synthesize amphiphilic block copolymers comprising one hydrophilic block with LCST characteristics.[14] PBA and poly(dimethylsiloxane) were chosen as hydrophobic blocks. As for the hydrophilic block, *N*-isopropyl acrylamide (NIPAM) was polymerized either alone or in combination with acrylamide or a hydrophobic comonomer. It was demonstrated that the cloud point of the block copolymer could be efficiently controlled by the proper choice of the composition of the thermosensitive block. As a result, these thermoresponsive amphiphilic block copolymers were evaluated as costabilizers for stimulable oil-in-water emulsions. It appeared that the critical temperature for the reversible precipitation−redissolution of the emulsion perfectly matches that of the block copolymer taken alone.[14]

Besides the self-organizing properties of these amphiphilic block copolymers in bulk or at interfaces, associations of thermoresponsive macromolecules with nanoparticles (NPs) have attracted growing interest in recent years.[15] Combining the two systems allows one to build new "smart" nanocomposites having the quite unique properties of the NPs (in catalysis, optics, electronics, etc.)[16] and the thermosensitivity related to the copolymer. For example, elaboration of thermoresponsive silica NPs,[17] palladium NPs,[18] iron oxide NPs,[19] and quantum dots[20] have been described.

Among all those hybrid systems, AuNPs@PNIPAM composites have been extensively studied in the past decade.[21] Syntheses were carried out either by growth of the NPs within PNIPAM particles,[22] grafting of the polymer on preformed NPs,[23] trapping of the NPs within PNIPAM microgels,[24] or by simple physical adsorption of the polymer on the NPs surface.[25] Adsorption of amphiphilic compounds (polymers or surfactants) on NPs may be more efficient with larger hydrophobic groups. This has been clearly demonstrated in the case of Pluronic polymers[26] and bolaamphiphiles[27] on AuNPs. Therefore, copolymers comprising a PNIPAM block and another more hydrophobic block may induce a stronger adsorption on NPs and favor the formation of


(9) (a) Bendejacq, D.; Ponsinet, V.; Joanicot, M.; Vacher, A.; Airiau, M. *Macromolecules* **2003**, *36*(19), 7289–7295. (b) Jacquin, M.; Muller, P.; Lizarraga, G.; Bauer, C.; Cottet, H.; Theodoly, O. *Macromolecules* **2007**, *40*(8), 2672–2682.

(10) Gerardin, C.; Sanson, N.; Bouyer, F.; Fajula, F.; Putaux, J. L.; Joanicot, M.; Chopin, T. *Angew. Chem., Int. Ed.* **2003**, *42*(31), 3681–3685.

(11) Yokota, K.; Morvan, M.; Berret, J. F.; Oberdisse, J. *Europhys. Lett.* **2005**, *69*(2), 284–290.

(12) Theodoly, O.; Jacquin, M.; Muller, P.; Chhun, S. *Langmuir* **2009**, *25*(2), 781–793.

(13) Destarac, M.; Deroo, S.; Lannibois-Dréan, H.; Sénéchal, A.; Bzducha, W. MADIX Technology: from Innovative Concepts to Industrialization of Block Copolymers for Emulsion Stabilization. In *Controlled/Living Radical Polymerization: Progress in RAFT, DT, NMP and OMRP*; Matyjaszewski, K., Ed.; American Chemical Society: Washington, D.C., 2009; Vol. *1024*, p 347.

(14) Destarac, M.; Papon, A.; Van Gramberen, E.; Karagianni, K. *Aust. J. Chem.* **2009**, *62*(11), 1488–1491.

(15) (a) Liu, R. X.; Fraylich, M.; Saunders, B. R. *Colloid Polym. Sci.* **2009**, *287*(6), 627–643. (b) Smith, A. E.; Xu, X. W.; McCormick, C. L. *Prog. Polym. Sci.* **2010**, *35*(1−2), 45–93.

(16) (a) Burda, C.; Chen, X. B.; Narayanan, R.; El-Sayed, M. A. *Chem. Rev.* **2005**, *105*(4), 1025–1102. (b) Gao, J. H.; Gu, H. W.; Xu, B. *Acc. Chem. Res.* **2009**, *42*(8), 1097–1107. (c) Murphy, C. J.; Gole, A. M.; Stone, J. W.; Sisco, P. N.; Alkilany, A. M.; Goldsmith, E. C.; Baxter, S. C. *Acc. Chem. Res.* **2008**, *41*(12), 1721–1730.

(17) (a) Wang, H. J.; Peng, M.; Zheng, J.; Li, P. J. *Colloid Interface Sci.* **2008**, *326*(1), 151–157. (b) Wu, T.; Zhang, Y. F.; Wang, X. F.; Liu, S. Y. *Chem. Mater.* **2008**, *20*(1), 101–109.

(18) Li, D. J.; Dunlap, J. R.; Zhao, B. *Langmuir* **2008**, *24*(11), 5911–5918.

(19) (a) Yuan, Q.; Venkatasubramanian, R.; Hein, S.; Misra, R. D. K. *Acta Biomater.* **2008**, *4*(4), 1024–1037. (b) Zhang, S. M.; Zhang, L. N.; He, B. F.; Wu, Z. S. *Nanotechnology* **2008**, *19*(32), 325608.

(20) Janczewski, D.; Tomczak, N.; Han, M. Y.; Vancso, G. J. *Eur. Polym. J.* **2009**, *45*(7), 1912–1917.

(21) (a) Karg, M.; Hellweg, T. *Curr. Opin. Colloid Interface Sci.* **2009**, *14*(6), 438–450. (b) Feng, M.; Chen, Y.; Gu, L. L.; He, N.; Bai, J. R.; Lin, Y.; Zhan, H. B. *Eur. Polym. J.* **2009**, *45*(4), 1058–1064.

(22) (a) Kim, J. H.; Lee, T. R. *Langmuir* **2007**, *23*(12), 6504–6509. (b) Suzuki, D.; Kawaguchi, H. *Langmuir* **2005**, *21*(18), 8175–8179.

(23) (a) Contreras-Caceres, R.; Pacifico, J.; Pastoriza-Santos, I.; Perez-Juste, J.; Fernandez-Barbero, A.; Liz-Marzan, L. M. *Adv. Funct. Mater.* **2009**, *19*(19), 3070–3076. (b) Alvarez-Puebla, R. A.; Contreras-Caceres, R.; Pastoriza-Santos, I.; Perez-Juste, J.; Liz-Marzan, L. M. *Angew. Chem., Int. Ed.* **2009**, *48*(1), 138–143.

(24) Budhlall, B. M.; Marquez, M.; Velev, O. D. *Langmuir* **2008**, *24*(20), 11959–11966.

(25) Kang, Y. J.; Taton, T. A. *Angew. Chem., Int. Ed.* **2005**, *44*(3), 409–412.

(26) (a) Rahme, K.; Gauffre, F.; Marty, J. D.; Payre, B.; Mingotaud, C. *J. Phys. Chem. C* **2007**, *111*(20), 7273–7279. (b) Rahme, K.; Oberdisse, J.; Schweins, R.; Gaillard, C.; Marty, J. D.; Mingotaud, C.; Gauffre, F. *ChemPhysChem* **2008**, *9*(15), 2230–2236.

(27) Sistach, S.; Rahme, K.; Perignon, N.; Marty, J. D.; Viguerie, N. L. D.; Gauffre, F.; Mingotaud, C. *Chem. Mater.* **2008**, *20*(4), 1221–1223.

hybrid composites in water. Furthermore, the critical temperature characteristics of the polymer/NP system can be easily adjusted by using such a copolymer instead of the PNIPAM homopolymer. Indeed, the thermal response of a PNIPAM-based copolymer depends on its exact composition.[28]

Herein, we report the synthesis and characterization of PBA-*b*-PNIPAM block copolymers, the study of their thermoresponsive behavior and their use as stabilizing agent of AuNPs to yield thermosensitive nanohybrids.

## 2. Materials and methods

**2.1. Reagents.** Tetrachloroauric acid trihydrate ($HAuCl_4$, $3H_2O$), sodium borohydride ($NaBH_4$), sodium chloride (NaCl), sodium hydroxide (NaOH), and 1-hexadecanethiol were purchased from Aldrich Fine chemicals and were used without further purification. *N*-isopropylacrylamide (99%, NIPAM) and *n*-butyl acrylate (99%, BA) were supplied from Acros Organics. BA was filtered over alumina to remove inhibitor prior to polymerization. The *O*-ethyl-*S*-(1-methoxycarbonyl) ethyldithiocarbonate MADIX/RAFT agent (Rhodixan A1) was obtained from Rhodia and use as received. The 2,2′-azobis-(isobutyronitrile) initiator (98%, AIBN) was purchased from Janssen Chimica and recrystallized from ethanol before use. Absolute ethanol (AnalaR normapur VWR) was used as received. Using a Purite device, water was purified through a filter and ion-exchange resin (resistivity ≈16 MΩ cm).

**2.2. Characterization.** *2.2.1. Size Exclusion Chromatography* (*SEC*). Average number molecular weights ($M_n$) and polydispersity indexes (PDI) were determined by SEC on an apparatus equipped with a Waters 2140 refractive index (RI) detector, using a Waters Styragel HR 4E column (eluent, THF; flow rate, 1 mL $min^{-1}$). Molecular weights were calculated on the basis of polystyrene standards. Typically, samples at a concentration of ca. 10 mg $mL^{-1}$ in THF were injected. Alternatively, samples were analyzed with a SEC apparatus comprising a Varian ProStar 325 UV detector (dual wavelength analysis) and a Waters 410 refractive index detector, using two Shodex K-805 L columns (8 mm ×300 mm, 13 μm) and DMF + LiCl (0.1 N) as the eluent at 40 °C (flow rate, 1 mL $min^{-1}$). This system was calibrated using narrow poly(methyl methacrylate) standards ranging from 900 to 625 000 g $mol^{-1}$.

*2.2.2. Differential Scanning Calorimetry* (*DSC*). The glass transition temperatures of the polymers were determined with a temperature increase rate of 10 °C $min^{-1}$ using a Perkin-Elmer PYRIS 1 calorimeter.

$^1H$ and $^{13}C$ NMR spectra were recorded on a Bruker ARX 400 at 400.13 MHz and at 100.61 MHz, respectively.

*2.2.3. Interfacial Tension*. Measurements of the surface tension were performed at 25 °C using the Wilhelmy plate method with a tensiometer (Kruss K20 Easy Dyne).

*2.2.4. Determination of Cloud Points*. Transmittance of polymer aqueous solutions was recorded with a HP 8452A diode array spectrophotometer with increasing temperature at different heating rates. The cloud points were then calculated by the extrapolation to 0 °C $min^{-1}$ of the cloud points obtained from the inflection point of each transmittance curve. Three independent measurements were performed for each sample.

*2.2.5. Dynamic Light Scattering Measurements* (*DLS*). DLS measurements were carried out at different temperatures with a Malvern Instrument Nano-ZS equipped with a He−Ne laser ($\lambda$ = 633 nm). Samples were introduced into cells (pathway: 10 mm) after filtration through 0.45 μm PTFE microfilters. The correlation function was analyzed via the general purpose method (NNLS) to obtain the distribution of diffusion coefficients ($D$) of the solutes, and then the apparent equivalent hydrodynamic diameter ($\langle D_h \rangle$) was determined using the Stokes−Einstein equation. Mean diameter values were obtained from three different runs. Standard deviations were evaluated from hydrodynamic diameter distribution.

*2.2.6. Transmission Electron Microscopy* (*TEM*). A drop of the aqueous dispersion was placed on a carbon-coated copper TEM grid and left to dry under air. For samples needing negative staining, the TEM grid was successively placed on a drop of the sample solution for 2 min, on a drop of an aqueous solution of uranyl acetate (2 wt %, 2 min) and finally on a drop of distilled water, after which the grid was then air-dried before introduction into the electron microscope. To visualize mesoglobules, we heated polymer solutions (45 °C) for 1 h prior to the deposit. The previously described procedure for preparation of TEM grids was then employed; however, they were dried in an oven at 45 °C. The samples were viewed with a HITACHI HU12 operating at 70 kV. Size distribution was determined by manual counting on ca. 150 particles, using WCIF Image J software.

*2.2.7. Small-Angle Neutron Scattering* (*SANS*). SANS experiments were performed with the PACE spectrometer at the Orphée reactor (LLB, Saclay). Polymer solutions in $D_2O$ solvent were put inside quartz cells of 2 mm gap and measured at 20 and 40 °C. Different spectrometer configurations were used: a neutron wavelength ($\lambda$) of 7 Å with a sample to detector distance of 3 m to obtain intermediate q value range, a wavelength of 7 Å with a distance of 1 m to reach high q values and a wavelength of 17 Å and 4.8 m to reach low $q$ values required to observe large objects. The neutron wavelength distribution $\Delta\lambda/\lambda$ was 0.11. The incident collimation was obtained from two circular holes, one close to the sample with a 7 mm diameter and the second one of either 16 mm diameter, 2.5 m apart from the sample diaphragm for the two highest q domains, or of 12 mm diameter, 5 m apart from the sample diaphragm for the smallest q range. The scattering vector range thus reached was

(28) (a) Soutar, I.; Swanson, L.; Adamson, P. G.; Flint, N. J. *Macromolecules* **2009**, *42*(22), 9153–9160. (b) Vieira, N. A. B.; Neto, J. R.; Tiera, M. J. *Colloids Surf., A* **2005**, *262*(1−3), 251–259. (c) Chee, C. K.; Rimmer, S.; Shaw, D. A.; Soutar, I.; Swanson, L. *Macromolecules* **2001**, *34*(21), 7544–7549.

$0.0025 < q\,(\text{Å}^{-1}) < 0.35$. Scattering intensities have also been normalized by the incoherent signal delivered by a 1 mm gap water sample in order to account for efficiency of detector cells.[29] Absolute values of the scattering intensity, $I(q)$ in $\text{cm}^{-1}$, were obtained from the direct determination of the number of neutrons in the incident beam and the detector cell solid angle.[30] No background was subtracted to the copolymer sample scattering, thus a flat incoherent signal is observed at high q values. The scattering curves of diluted copolymer solutions have been fitted to the model of polydisperse spheres (diameter $D$) by using a Gaussian distribution of diameter ($\sigma_D$), and taking into account for each spectrometer configuration the convolution with the corresponding resolution function.[31]

**2.3. Synthesis.** *2.3.1. Block Copolymers Synthesis.* A typical procedure for synthesizing block copolymers of BA and NIPAM is as follows: 51 mg of AIBN, 0.521 g of Rhodixan A1, 4.994 g of BA, and 3.39 g of ethanol are placed in a two-neck, round-bottomed flask equipped with a magnetic stirrer and a reflux condenser. The solution is then degassed for 15 min by bubbling argon. It is then heated at 75 °C for 3 h, keeping a slow stream of argon in the reactor. After this period of time, the solution is cooled to ambient temperature and the polymer is analyzed. BA conversion > 99% ($^1$H NMR); $M_n = 2250$ g mol$^{-1}$, PDI = 1.55 (given by SEC in THF); 3.873 g of the obtained PBA is mixed with 187 mg of AIBN, 15.56 g of NIPAM, and 16.45 g of ethanol. The solution is then degassed for 15 min by bubbling argon. It is then heated at 75 °C during nine hours, keeping a slow stream of argon in the reactor. The reaction mixture is then cooled down to ambient temperature and the polymer is analyzed. NIPAM conversion > 99% ($^1$H NMR); $M_n = 7350$ g mol$^{-1}$, PDI = 1.29 (given by SEC in THF).

*2.3.2. Micelle Formation.* Concentrated solutions (20 wt %) of amphiphilic block copolymers were prepared in ethanol or in methanol-$d_4$, which are good solvents for both blocks. Then, these solutions were added dropwise to an adequate amount of water or $D_2O$ with vigorous stirring. The final content in ethanol or in methanol-$d_4$ was equal to or less than 1% v/v, and it was accepted as negligible.

*2.3.3. AuNP Formation.* Preformed NPs were synthesized as previously described.[27,32] Briefly, to 5 mL of a $1 \times 10^{-2}$ mol L$^{-1}$ $HAuCl_4$ solution were added 94 mL of distilled water and 250 $\mu$L of a 1 mol L$^{-1}$ aqueous solution of sodium hydroxide. The pH was then adjusted (if necessary) around 7.5−8 and 500 $\mu$L of a fresh $NaBH_4$ solution (0.1 mol L$^{-1}$) were subsequently added under manual stirring. The solution color immediately turned into dark red, indicating the formation of AuNPs. Typical TEM analysis of these NPs is given as Supporting Information (Figure S4).

*2.3.4. Coating of the Preformed Nanoparticles.* Typically, for a final polymer concentration of 0.1 wt %, 0.9 mL of desionized water and 0.1 mL of a 1 wt % aqueous stock solution of polymer were added to 1 mL of a $5 \times 10^{-4}$ mol L$^{-1}$ aqueous Au NPs stock solution to yield coated NPs.

*2.3.5. In situ Synthesis of AuNPs.*[33] The amount of $PBA_{2k}$-*b*-$PNIPAM_{8k}$ was adjusted as a function of the final desired polymer concentration. Typically, 380 $\mu$L of deionized water was added to 1.5 mL of 0.2 wt % $PBA_{2k}$-*b*-$PNIPAM_{8k}$ aqueous solution followed by the addition of 100 $\mu$L of 0.01 mol L$^{-1}$ $HAuCl_4$ aqueous solution. Then, NaOH aqueous solution was added to adjust the pH to 8 and the mixture was heated in an oven at 20 or 45 °C for 15 min. Finally, 10 $\mu$L of freshly prepared 0.1 mol L$^{-1}$ $NaBH_4$ solution was added. The mixture color turned into brown, red, or light orange, at different rates, depending on $PBA_{2k}$-*b*-$PNIPAM_{8k}$ concentration.

## 3. Results and Discussion

**3.1. Synthesis and Characterization of Block Copolymers.** MADIX/RAFT block copolymers of BA and NIPAM were synthesized via two-step polymerizations initiated by 2,2′-azobis(isobutyronitrile) in ethanol at 75 °C in the presence of the *O*-ethyl-*S*-(1-methoxycarbonyl)ethyldithiocarbonate MADIX agent (Rhodixan A1), without purification of the intermediate PBA block (Scheme 1).

PBA-*b*-PNIPAM copolymers with targeted structures corresponding to $PBA_{2k}$-*b*-$PNIPAM_{8k}$ and $PBA_{5k}$-*b*-$PNIPAM_{5k}$ (2k and 5k for a theoretical $M_n$ of the PBA block equal to 2000 and 5000 g mol$^{-1}$ respectively) were selected. Reaction conditions were chosen so that the $^1$H NMR analysis confirmed that the BA and NIPAM conversions were greater than 99% for each polymerization step and for the two block copolymers. The transfer constant to xanthate ($C_X$) and interchain transfer constant ($C_{ex}$) respectively influence the $M_n$ evolution profile and polydispersity index during polymerization.[34] Jacquin et al. determined a $C_X$ value equal to 2.7 for Rhodixan A1 in BA polymerization in ethanol.[9b] We determined experimentally a transfer constant to Rhodixan A1 ($C_X$) equal to 3.3 ± 0.5 for NIPAM polymerization in ethanol by plotting the monomer concentration vs transfer agent concentration with a double log scale,[35] after both concentrations were followed by high performance liquid chromatography. In MADIX/RAFT polymerizations for which the contribution of initiator-derived chains and side reactions like transfer to solvent are negligible, the control of $M_n$ at the end of the polymerization (~99% monomer conversion) is obtained if $C_X$ is greater than 1.

(29) Brulet, A.; Lairez, D.; Lapp, A.; Cotton, J. P. J. *Appl. Crystallogr.* **2007**, *40*, 165–177.
(30) Cotton, J. P. In *Neutron, X-ray and Light Scattering*; Lindler, P., Zemb, T., Eds.; North-Holland: Amsterdam, 1991; p 19.
(31) (a) Pedersen, J. S. *J. Phys. IV* **1993**, *3*(C8), 491–498. (b) Lairez, D. *J. Phys. IV* **1999**, *9*(P1), 67–81.
(32) Keilitz, J.; Radowski, M. R.; Marty, J. D.; Haag, R.; Gauffre, F.; Mingotaud, C. *Chem. Mater.* **2008**, *20*(7), 2423–2425.
(33) Perignon, N.; Mingotaud, A. F.; Marty, J. D.; Rico-Lattes, I.; Mingotaud, C. *Chem. Mater.* **2004**, *16*(24), 4856–4858.
(34) Chong, Y. K.; Krstina, J.; Le, T. P. T.; Moad, G.; Postma, A.; Rizzardo, E.; Thang, S. H. *Macromolecules* **2003**, *36*(7), 2256–2272.
(35) Guinaudeau, A. PhD thesis, University of Toulouse, Toulouse, France, **2010**.

**Scheme 1. Synthesis of Poly(*n*-butyl acrylate)-*b*-poly(*N*-isopropyl acrylamide), PBA-*b*-PNIPAM, by MADIX/RAFT Polymerization, Self-Assembly in Aqueous Solutions, and Thermoinduced Aggregation**

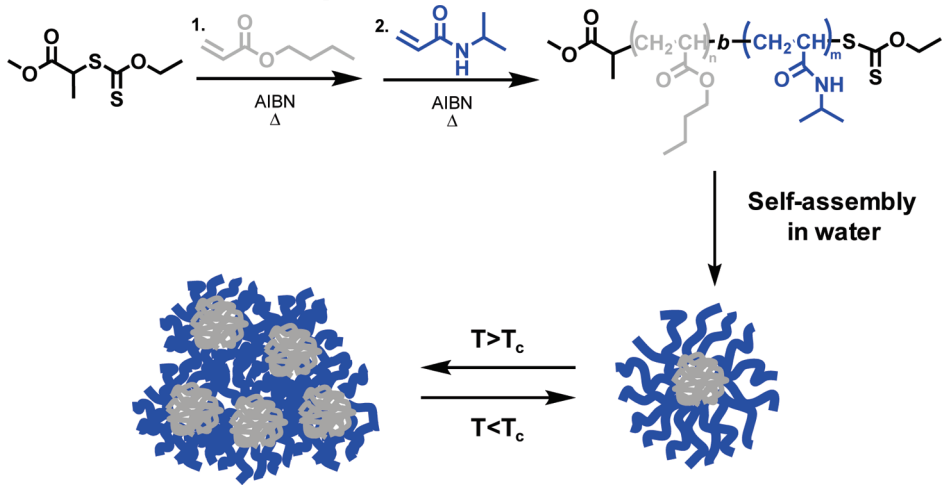


**Table 1. Characteristics of Polymer Samples: $M_n$, Polydispersity Indexes, and Glass Transition Temperatures ($T_g$)**

| | $M_n$ (g mol$^{-1}$) | PDI | $T_g$ (°C) | $\Delta C_p$ (J g$^{-1}$) |
|---|---|---|---|---|
| $PNIPAM_{8k}$ | 17600[a] | 1.27[a] | 127.9 | 0.4 |
| $PNIPAM_{10k}$ | 21 300[a] | 1.31[a] | n.d. | n.d . |
| $PBA_{2k}$ | 2300[b] | 1.55[b] | −50.7 | 0.5 |
| $PBA_{2k}$-*b*-$PNIPAM_{8k}$ | 15 300[a] | 1.30[a] | 108.9 | 0.2 |
| | 7400[b] | 1.29[b] | | |
| $PBA_{5k}$ | 5100[b] | 1.58[b] | n.d. | n.d. |
| $PBA_{5k}$-*b*-$PNIPAM_{5k}$ | 8400[a] | 1.20[a] | −48.0 | 0.1 |
| | 6100[b] | 1.53[b] | 106.7 | 0.2 |

[a] SEC in DMF; calibration PMMA. [b] SEC in THF; calibration PS.

This is confirmed for PBA as shown in Table 1 (entries 3 and 5) when $M_n$ is determined by SEC in THF. The $M_n$ values of PBA samples could not be determined by SEC in DMF because their elution volume was out of the PMMA calibration range, in the region typical of low molecular weight molecules, which means that the hydrodynamic volume of PBA is smaller than that of PMMA in the DMF eluent. The $M_n$ of PNIPAM synthesized in the presence of Rhodixan A1 in ethanol was nearly twice as high as the theoretical $M_n$ value (entries 1 and 2 of Table 1) when SEC was performed in DMF. We attributed these differences in $M_n$ to differences in hydrodynamic volumes between PMMA and PNIPAM in the DMF eluent, as the $C_X$ value of 3.3 for NIPAM rules out the possibility for the xanthate to be partially reacted at the end of the polymerization. The PDIs reported in Table 1 lie in the 1.5−1.6 range for PBA and are close to 1.3 for PNIPAM. As PDI can be approximated to $1 + 1/C_{ex}$ at the end of the polymerization,[36] it can be estimated that the xanthate interchain transfer is relatively slow in both cases, and faster in the case of NIPAM than for BA. The experimental $M_n$ values of the copolymers are slightly lower than theoretical estimations when SEC is performed in THF. For a given theoretical $M_n$ of 10k for the two block copolymers of entries 4 and 6 in Table 1, it appears that the $M_n$ value determined by SEC in DMF with PMMA standards is strongly dependent on the composition of the copolymer. This can again be explained by the significant differences in hydrodynamic volumes of PBA and PNIPAM in the DMF eluent. The PDIs of the block copolymers tend to slightly decrease compared to that of the PBA block after NIPAM polymerization ($1.20 < PDI < 1.53$). Most importantly, the overlay of SEC chromatograms in THF of the PBA precursor and resulting diblock copolymers show that in both cases, the PBA was fully incorporated in the final copolymer (Figure 1). Differential scanning calorimetry (DSC) analysis was performed for all homopolymers and diblock copolymers. The thermograms showed glass transition temperatures at around 108.9 °C for $PBA_{2k}$-*b*-$PNIPAM_{8k}$ and −48.0 and 106.7 °C for $PBA_{5k}$-*b*-$PNIPAM_{5k}$. These transitions were attributed to the glass transition temperature of PBA (−50.7 °C) and PNIPAM (127.9 °C), which suggests that phase separation of the two blocks is occurring in the solid state. Because the PBA content is very low in the case of the first block copolymer, the transition corresponding to the PBA could not be observed on DSC analysis.

**3.2. Properties of Aqueous Solutions of Block Copolymers.** *3.2.1. Self-Assembly in Water at 20 °C.* When amphiphilic block copolymers are dissolved in water, they tend to aggregate in order to decrease the free energy of the system by the formation of an "interface" between "oily" cores and water (the so-called hydrophobic effect).[37] However, the self-assembly in regular spherical micelles is not always observed and, sometimes, nonequilibrium nanostructures are obtained.[38] Indeed, the preparation method has an important influence on the aggregate nanostructure.[39] When the block copolymers $PBA_{2k}$-*b*-$PNIPAM_{8k}$ and $PBA_{5k}$-*b*-$PNIPAM_{5k}$ were directly solubilized in water, micellar aggregates with a relatively large distribution of sizes could be observed

(36) Muller, A. H. E.; Zhuang, R. G.; Yan, D. Y.; Litvinenko, G. *Macromolecules* **1995**, *28*(12), 4326–4333.
(37) Chandler, D. *Nature* **2005**, *437*(7059), 640–647.
(38) Yu, K.; Zhang, L. F.; Eisenberg, A. *Langmuir* **1996**, *12*(25), 5980–5984.
(39) Riess, G. *Prog. Polym. Sci.* **2003**, *28*(7), 1107–1170.

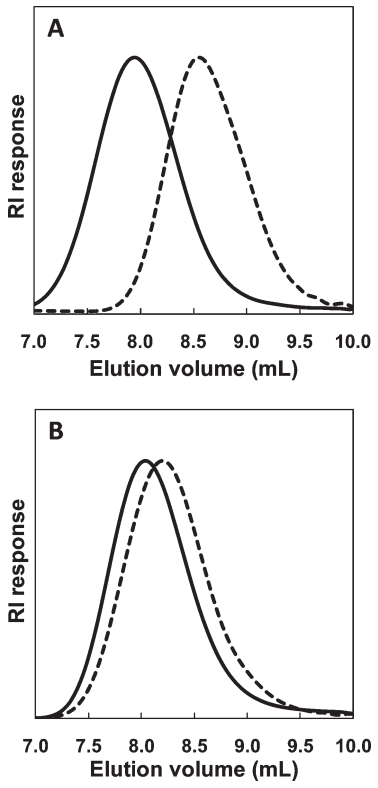


**Figure 1.** Size exclusion chromatograms (RI response) in THF of (A) $PBA_{2k}$ (dotted line) and $PBA_{2k}$-*b*-$PNIPAM_{8k}$ (solid line) and (B) $PBA_{5k}$ (dotted line) and $PBA_{5k}$-*b*-$PNIPAM_{5k}$ (solid line).

by DLS. So, a solvent-assisted method was employed in which the block copolymers were first solubilized in ethanol and then transferred to water. It is worth to note that the micelles were prepared with a slightly different procedure than usually described in the literature. In most works, water is slowly added to the solution of block copolymer in an organic solvent, gradually changing the quality of the solvent. Though, in our case, this method leaded to micelles that were largely distributed.

Because ethanol is a good solvent for both blocks, the block copolymers are molecularly dissolved as random coils in ethanol solutions, presenting average hydrodynamic diameters ($\langle D_h \rangle$) on the order of 4−5 nm, exactly as PNIPAM homopolymers (Table 2). When these block copolymers were transferred from organic solvent into aqueous solutions, a significant increase in the diameters was observed by DLS, whereas only a slight change was seen for homopolymers (Table 2), suggesting that they self-assembled in micelles. In fact, TEM images of dried aqueous solutions show very regular monodisperse spherical micelles (Figure 2) with diameters agreeing with DLS results. As expected, the diameters measured by TEM are slightly lower than those observed by DLS because they correspond to gyration diameters rather than hydrodynamic diameters. These results were further confirmed by SANS measurements presented in Figure 3. These SANS curves were well-fitted to the simple model of polydisperse sphere, which gave us the mean micelle diameter and its distribution (Table 2).

At 20 °C, the micelles sizes of $PBA_{5k}$-*b*-$PNIPAM_{5k}$ are more than twice those of $PBA_{2k}$-*b*-$PNIPAM_{8k}$: this ratio roughly corresponds to the ratio of hydrophobic block lengths of these two copolymers. Such an increase of micelle size, proportional to the length of the hydrophobic block, would correspond to the strong aggregation limit case predicted for the aggregation of diblock copolymer, which has been observed in various diblock copolymers.[40] In such systems, the core contains practically only the hydrophobic blocks. Thus, when the hydrophobic block is longer, the formed micelles will have a higher aggregation number, leading to an increase in the micelle size.

In this case, the corona (the PNIPAM blocks) surrounding the core (the PBA blocks) is also swollen by the solvent. Its contribution to the SANS signal is very weak. Thus, with this assumption, the micelle diameter deduced from SANS is the diameter of the hydrophobic PBA core alone. The average aggregation number $N_{agg}$ in the micelles can be determined from the size of the core ($R_{core}$), the mean average molar mass in weight of the core block ($M_{core}$) and the block density inside the core ($\rho_{core}$ = 1.1 g cm$^{-3}$, assuming a dense and solvent excluded core) using the following expression:

$$N_{agg} = 4\pi\rho_{core}R_{core}^3 N_{Av}/3M_{core}$$

With $M_{core} = M_{PBA}$ and $N_{Av}$ = Avogadro's number, we obtain $N_{agg}$ = 710 and 4800, respectively, for copolymer micelles from $PBA_{2k}$-*b*-$PNIPAM_{8k}$ and $PBA_{5k}$-*b*-$PNIPAM_{5k}$, in agreement with the expected scaling law $N_{agg} \propto N_A^2$ ($N_A$ being the number of monomers of the hydrophobic block). The surface area per chain $A_c = 4\pi R_{core}^2/N_{agg}$ calculated for the two micellar systems gives values of 1.13 and 1.10 nm$^2$, respectively, which are also in good agreement with the estimated surface occupied by one NIPAM monomer. Critical aggregation concentration were determined from interfacial tension measurements and found around $3 \times 10^{-4}$ wt % for both copolymers (see the Supporting Information, Figure S1).

*3.2.2. Thermosensitive Behavior*. Cloud points ($T_c$) of aqueous solutions of PNIPAM homopolymers and PBA-*b*-PNIPAM block copolymers were determined by turbidimetry. A hysteresis between the heating process and the cooling process could be observed for all solutions, which was accentuated for higher heating/cooling rates (see the Supporting Information, Figure S2). At a heating/cooling rate of 0.1 °C min$^{-1}$, the cloud points obtained while cooling were 2−3 °C lower than the cloud points observed while heating. This phenomenon had already been observed for PNIPAM polymers, even in very dilute solutions, and can be explained by the fact that the swelling of the compact aggregates formed at higher temperatures is relatively difficult because of the intrachain entanglement.[41] Cloud point temperature was found at 36.5 °C, which is close to cloud points values observed for PNIPAM

(40) Forster, S.; Zisenis, M.; Wenz, E.; Antonietti, M. *J. Chem. Phys.* **1996**, *104*(24), 9956–9970.
(41) Wang, X. H.; Qiu, X. P.; Wu, C. *Macromolecules* **1998**, *31*(9), 2972–2976.
(42) Xia, Y.; Burke, N. A. D.; Stover, H. D. H. *Macromolecules* **2006**, *39*(6), 2275–2283.

**Table 2. Cloud Points ($T_c$) and DLS, TEM, and SANS Data on Polymer Aqueous Solutions at 20 and 40 °C (0.2 wt %)[a]**

| | | 20 °C | | | | 40 °C | | |
|---|---|---|---|---|---|---|---|---|
| polymer | $T_c$ (°C) | $\langle D_h \rangle_{EtOH}$ (nm) (20 wt %) | $\langle D_h \rangle_{water}$ (nm) | $\langle D \rangle_{TEM}$ (nm) | $\langle D \rangle_{SANS}$ (nm) (PBA core) | $\langle D_h \rangle_{water}$ (nm) | $\langle D \rangle_{TEM}$ (nm) | $\langle D \rangle_{SANS}$ (nm) |
| $PNIPAM_{10k}$ | 36.5 | 4.7 ± 0.9 | 6 ± 4 | | | 486 ± 194 | | |
| $PBA_{2k}$-*b*-$PNIPAM_{8k}$ | 29.9 | 4.6 ± 2.3 | 28 ± 6 | 22 ± 3 | 16 ± 2 | 114 ± 5 | | 104 ± 15 |
| $PBA_{5k}$-*b*-$PNIPAM_{5k}$ | 28.1 | 4.6 ± 0.6 | 62 ± 12 | 41 ± 10 | 41 ± 7 | 132 ± 1 | | 106 ± 17 |

[a] Note: Errors in DLS measurements were calculated by multiplying polydispersity values by the mean hydrodynamic diameter values.

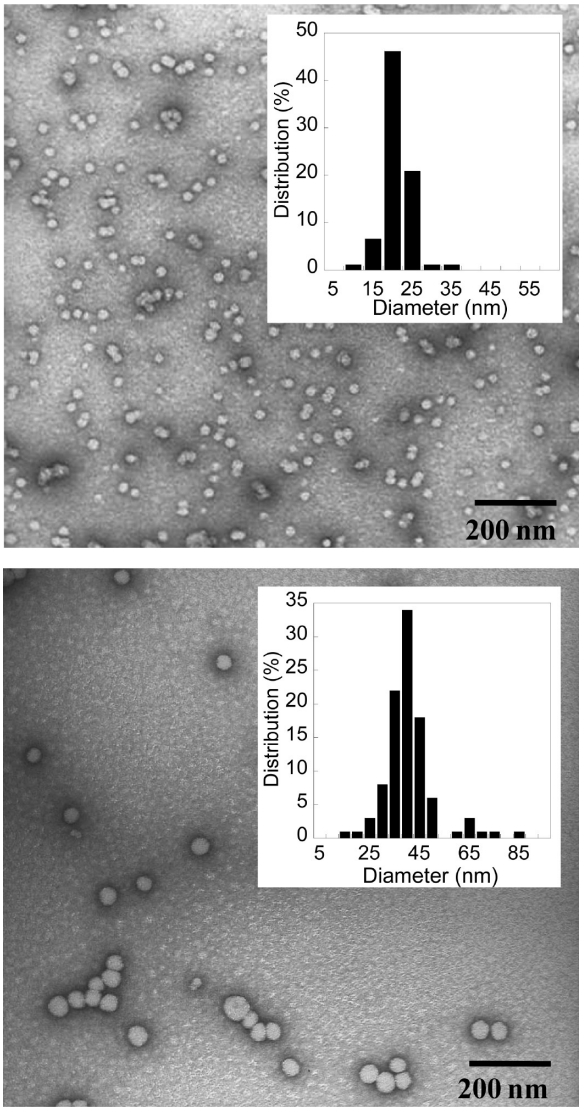


**Figure 2.** TEM images and distribution of aggregates of $PBA_{2k}$-*b*-$PNIPAM_{8k}$ (top) and $PBA_{5k}$-*b*-$PNIPAM_{5k}$ (bottom).

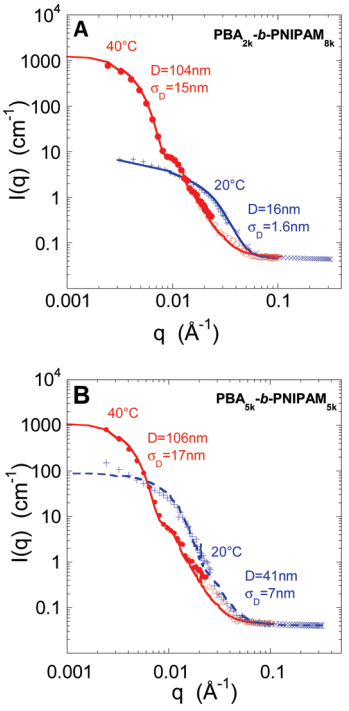


**Figure 3.** Scattering intensity in absolute units ($cm^{-1}$) of $D_2O$ solutions of (A) $PBA_{2k}$-*b*-$PNIPAM_{8k}$ (0.2 wt %) and (B) $PBA_{5k}$-*b*-$PNIPAM_{5k}$, measured at 20 °C (blue +, blue ×) and at 40 °C (red ○, red ●). Lines are the best fits to a model of polydisperse sphere (mean diameter D, standard deviation $\sigma_D$) taking into account the resolution function of the spectrometer.

with similar molecular weights obtained by controlled radical polymerization techniques.[42]

It is known that the incorporation of hydrophobic monomers on PNIPAM polymers modifies the hydrophilic/hydrophobic balance of the system, shifting the cloud point to lower temperature values.[28c] Here, we were able to modulate the cloud point of PNIPAM by the preparation of block copolymers with BA. Hence, $PBA_{2k}$-*b*-$PNIPAM_{8k}$ and $PBA_{5k}$-*b*-$PNIPAM_{5k}$ have cloud point values ca. 6 °C lower than PNIPAM homopolymers (Table 2 and Figure 4). In addition, the latter block copolymer exhibits a lower cloud point value ($T_c$ = 28.1 °C) than the former ($T_c$ = 29.9 °C) because of its greater BA content.

Another possibility for tuning the cloud points of these polymers is increasing the ionic strength of the polymer aqueous solutions. Salts are known to disrupt the hydration structure around the polymer, causing a decrease of the demixing temperature.[43] Indeed, a linear decrease in the cloud points of both $PNIPAM_{10k}$ and $PBA_{2k}$-*b*-$PNIPAM_{8k}$ was observed with increasing NaCl concentration (Figure 5). The influence in the salt concentration showed to be similar for both samples, leading to a decrease of more than 10 °C on the cloud point values at high NaCl concentration. Besides, the difference between the $T_c$ values of these two polymers remains practically constant up to a NaCl concentration of 0.5 mol $L^{-1}$.

(43) (a) Baltes, T.; Garret-Flaudy, F.; Freitag, R. *J. Polym. Sci., Part A: Polym. Chem.* **1999**, *37*(15), 2977–2989. (b) Van Durme, K.; Rahier, H.; Van Mele, B. *Macromolecules* **2005**, *38*(24), 10155–10163.

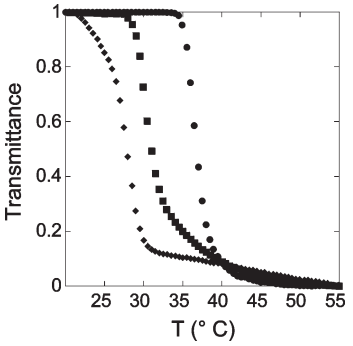


**Figure 4.** Transmittance vs temperature for 0.1 wt % aqueous solutions of $PNIPAM_{10k}$ (●), $PBA_{2k}$-*b*-$PNIPAM_{8k}$ (■), and 0.01 wt % aqueous solutions of $PBA_{5k}$-*b*-$PNIPAM_{5k}$ (♦) for a heating rate of 0.1 °C $min^{-1}$.

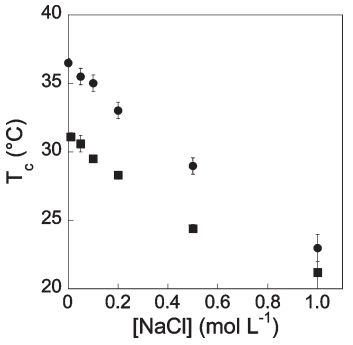


**Figure 5.** Cloud points of 0.1 wt % aqueous solutions of $PNIPAM_{10k}$ (●) and $PBA_{2k}$-*b*-$PNIPAM_{8k}$ (■) as a function of NaCl concentration.

*3.2.3. Formation of Mesoglobules.* When the block copolymers solutions were heated above their cloud point temperature, monodisperse aggregates of $PBA_{2k}$-*b*-$PNIPAM_{8k}$ and $PBA_{5k}$-*b*-$PNIPAM_{5k}$ with hydrodynamic diameters of 114 ± 5 nm and 132 ± 1 nm were detected by DLS, suggesting that stable dispersions of mesoglobules were formed (Table 2). An increase in copolymer concentration induces the formation of larger mesoglobules with quite a narrow distribution (see the Supporting Information, Figure S3a). Their formation was further confirmed by TEM experiments (negative staining) and SANS measurements. Indeed, when TEM deposit was performed above $T_c$, TEM images of $PBA_{2k}$-*b*-$PNIPAM_{8k}$ polymer solution showed spherical objects with a mean diameter of ca. 100 ± 40 nm (Figure 6). The large distribution observed by TEM might be caused by drying and/or the staining process, which leads to local overconcentration and, consequently, induces the formation of objects of different sizes. However, samples that were prepared using the same procedure at room temperature did not show such objects.

Because the mesoglobules appear to be spherical, it was consistent to fit the SANS data (see Figure 3) at 40 °C with the polydisperse hard sphere model, which gave a mean diameter of 104 ± 15 nm for $PBA_{2k}$-*b*-$PNIPAM_{8k}$ and 106 ± 17 nm for $PBA_{5k}$-*b*-$PNIPAM_{5k}$. At this temperature, PNIPAM was poorly solvated and both blocks contribute to scattering signal. This leads to similar mesoglobule sizes and an average $N_{agg}$ around 41 000 for both copolymers.

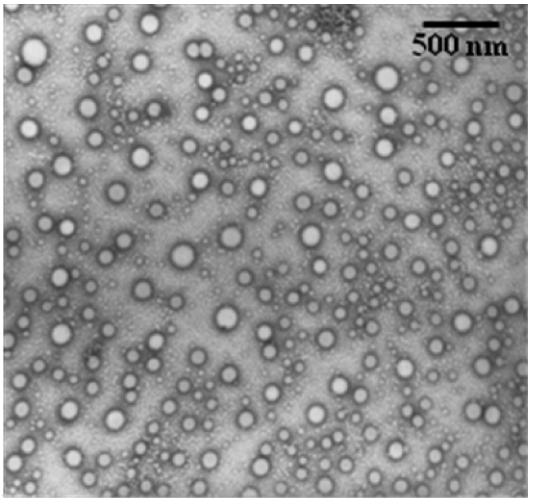


**Figure 6.** TEM images (negative stain) of mesoglobules formed above the cloud point temperature for $PBA_{2k}$-*b*-$PNIPAM_{8k}$.

Mesoglobules of PNIPAM homopolymers[44] as well as of hydrophobically modified PNIPAM polymers[45] have previously been observed. However, as far as we know, this is the first time that mesoglobules of PNIPAM-based amphiphilic block copolymers are detected. Although the reasons for the actual stability of these mesoglobules aggregates are still under debate, it is believed that it is due to the general features of the spinodal decomposition of polymer solutions and to the low probability of Brownian collisions in dilute solutions, which avoids the formation of larger aggregates that would precipitate in aqueous solutions.[44a] When the temperature is raised above the cloud point, polymer chains simultaneously undergo intrachain contraction and interchain association, giving rise to large aggregates that are loosely solvated by water molecules. These molecules are then ejected to bulk water, leading to the formation of very dense and rigid mesoglobules that cannot merge because of the very short contact time between two mesoglobules during a collision. Another explanation that has been suggested is that partial vitrification may take place within dense mesoglobules, decreasing the probability of merging.[46]

**3.3. Stabilization of AuNPs.** When a PNIPAM layer is physically or chemically attached to the surface of a Au NP, not only a steric stability is acquired for the NPs, but also the properties of the NPs can be controlled to some extent in response to any change in temperature. Moreover, incorporating well-defined polymers with desired molecular weight using the precision of MADIX/RAFT technology may be essential to better understand such modifications. Hence, coating of AuNPs using PNIPAM (or PNIPAM-based block copolymers) obtained by RAFT polymerization was extensively studied. Those

(44) (a) Kujawa, P.; Aseyev, V.; Tenhu, H.; Winnik, F. M. *Macromolecules* **2006**, *39*(22), 7686–7693. (b) Ye, J.; Xu, J.; Hu, J.; Wang, X.; Zhang, G.; Liu, S.; Wu, C. *Macromolecules* **2008**, *41*, 4416–4422.
(45) Kujawa, P.; Tanaka, F.; Winnik, F. M. *Macromolecules* **2006**, *39*, 3048–3055.
(46) Van Durme, K.; Verbrugghe, S.; Du Prez, F. E.; Van Mele, B. *Macromolecules* **2004**, *37*, 1054–1061.

nanohybrids were made either by a "grafting from"[47] or a "grafting to"[48] approach, or by direct growth of the NPs within PNIPAM particles.[49] Here, $PBA_{2k}$-*b*-$PNIPAM_{8k}$ and $PBA_{5k}$-*b*-$PNIPAM_{5k}$ amphiphilic block copolymers were adsorbed on the surface of preformed AuNPs. Properties of the obtained nanohybrids were compared to those of Au@PNIPAM with a similar molecular weight, allowing a better description of the nanohybrids formed. Those results were then compared to those obtained by in situ preparation of AuNPs. Lastly, stabilization properties of the nanohybrids were described.

*3.3.1. Coating of Preformed NPs.* To avoid any chemical modification of the polymers and to allow direct comparison of their stabilization properties, we separately synthesized AuNPs and subsequently mixed them with the polymer. AuNPs were synthesized by reduction of $HAuCl_4$ by $NaBH_4$.[32] Although no additional stabilizing agent was added, experimental conditions such as pH and gold precursor concentration have to be chosen carefully to obtain well-controlled AuNPs with good stabilization properties. First, the pH value of the $HAuCl_4$ needs to be adjusted around 8.0 before addition of $NaBH_4$ solution; in such conditions, $HAuCl_4$ was present mainly as $Au(OH)_4^-$ in solution[50] whose reduction favored the formation of AuNPs as single colloids. In addition, gold concentration need to be kept below $5 \times 10^{-4}$ mol $L^{-1}$ to avoid further aggregation of AuNPs (Supporting Information, Figure S4). The NPs dispersions obtained by this procedure exhibited a broad absorption band around 516 nm, resulting in a pink-red color of the dispersions. TEM measurements showed isolated AuNPs with an average diameter of approximately $8 \pm 2$ nm (see the Supporting Information, Figure S5). In addition, their hydrodynamic radius was found at $7.3 \pm 0.7$ nm, so they are present mainly as single colloid in aqueous solutions. Those NPs are negatively charged (due to the presence of chlorate and borate ions and hydroxyl derivatives at the surface of the NPs) with a zeta potential around $-30 \pm 2$ mV. Moreover, these AuNPs are stable in water with no significant change of optical properties over a month period (see the Supporting Information, Figure S6). Nevertheless, they are sensitive to any increase in ionic strength or change in pH, which induces a charge neutralization and subsequent aggregation. To stabilize these NPs, an adequate amount of polymer solution was added to AuNPs solutions to reach the final desired polymer concentration. These solutions were then analyzed to study the morphology and properties in solution of the obtained nanohybrids by UV−visible spectroscopy, DLS, and TEM measurements.

Amphiphilic polymers form micelles and other types of aggregates at concentrations higher than a critical value (critical aggregation concentration, CAC). The adsorption of polymers at the water/gas or water/solid interfaces, including the amount of adsorbed material as well as the structure of the adsorbed layer, is expected to be dependent on the types and amount of aggregates in solution. Micelles embedding NPs in their inner core are the most common systems described in literature.[51] Several examples of raspberry-like aggregates, with many particles in the corona region, are also described.[52]

We then investigated the effect of polymer concentration upon stabilization of the AuNPs. Dispersions of AuNPs stabilized by the diblock copolymers or the homopolymer $PNIPAM_{10k}$ were prepared at various polymer concentrations below and above the CAC. Destabilization was then induced by increasing the ionic strength of these solutions. Whereas non coated NPs solutions led to the formation of a dark precipitate, solutions of NPs stabilized by block copolymers remained unchanged even for polymer concentrations 10 orders of magnitude below the CAC. This result suggests that the stabilizing effect is not promoted by the bulk micelles formation. To probe the interactions of the different polymers with the AuNPs, we followed the maximum of the surface plasmon band (SPB) as a function of diblock copolymer concentration. For the bare AuNPs, its value was ca. 516 nm at 25 °C. When coated with $PBA_{2k}$-*b*-$PNIPAM_{8k}$, this value increased to ca. 520 nm and remained practically constant regardless of the copolymer concentration. This bathochromic shift of the maximum wavelength demonstrates the efficiency of copolymers to interact with the surface of AuNPs. Here, the block copolymers (Scheme 1) bear the xanthate group at the PNIPAM block chain end. The chemisorption of thiocarbonylthio groups to the surface of AuNPs was previously demonstrated and could be involved in the interaction between the polymer and the NPs surface.[53] Nevertheless, no changes in the SPB maximum wavelength of the nanohybrids were observed when the xanthate group of $PBA_{2k}$-*b*-$PNIPAM_{8k}$ was reduced to thiol before coating the AuNPs or when the reduction was carried out in the

(47) (a) Raula, J.; Shan, J.; Nuopponen, M.; Niskanen, A.; Jiang, H.; Kauppinen, E. I.; Tenhu, H. *Langmuir* **2003**, *19*(8), 3499–3504. (b) Zhang, W. A.; Liu, L.; Zhuang, X. D.; Li, X. H.; Bai, J. R.; Chen, Y. J. *Polym. Sci. A: Polym. Chem.* **2008**, *46*(21), 7049–7061. (c) Zhao, Y.; Perrier, S. *Macromolecules* **2007**, *40*(25), 9116–9124.

(48) (a) Boyer, C.; Bulmus, V.; Priyanto, P.; Teoh, W. Y.; Amal, R.; Davis, T. P. *J. Mater. Chem.* **2009**, *19*(1), 111–123. (b) Huang, Y. K.; Liu, Q.; Zhou, X. D.; Perrier, S.; Zhao, Y. L. *Macromolecules* **2009**, *42* (15), 5509–5517. (c) Liang, M.; Lin, I. C.; Whittaker, M. R.; Minchin, R. F.; Monteiro, M. J.; Toth, I. *ACS Nano* **2010**, *4*(1), 403–413. (d) Narain, R.; Gonzales, M.; Hoffman, A. S.; Stayton, P. S.; Krishnan, K. M. *Langmuir* **2007**, *23*(11), 6299–6304. (e) Yusa, S. I.; Fukuda, K.; Yamamoto, T.; Iwasaki, Y.; Watanabe, A.; Akiyoshi, K.; Morishima, Y. *Langmuir* **2007**, *23*(26), 12842–12848. (f) Zhao, J.; Shan, J.; Van Assche, G.; Tenhu, H.; Van Mele, B. *Macromolecules* **2009**, *42*(14), 5317–5327. (g) Zhu, M. Q.; Wang, L. Q.; Exarhos, G. J.; Li, A. D. Q. *J. Am. Chem. Soc.* **2004**, *126*(9), 2656–2657. (h) Boyer, C.; Whittaker, M. R.; Luzon, M.; Davis, T. P. *Macromolecules* **2009**, *42*(18), 6917–6926.

(49) (a) Aqil, A.; Qiu, H. J.; Greisch, J. F.; Jerome, R.; De Pauw, E.; Jerome, C. *Polymer* **2008**, *49*(5), 1145–1153. (b) Rezende, C. A.; Shan, J.; Lee, L. T.; Zalczer, G.; Tenhu, H. *J. Phys. Chem. B* **2009**, *113* (29), 9786–9794. (c) Shan, J.; Nuopponen, M.; Jiang, H.; Kauppinen, E.; Tenhu, H. *Macromolecules* **2003**, *36*(12), 4526–4533. (d) Shan, J.; Zhao, Y. M.; Granqvist, N.; Tenhu, H. *Macromolecules* **2009**, *42*(7), 2696–2701.

(50) Ivanova, S.; Petit, C.; Pitchon, V. *Appl. Catal., A* **2004**, *267*(1−2), 191–201.

(51) Sidorov, S. N.; Bronstein, L. M.; Kabachii, Y. A.; Valetsky, P. M.; Soo, P. L.; Maysinger, D.; Eisenberg, A. *Langmuir* **2004**, *20*(9), 3543–3550.

(52) Zheng, P.; Jiang, X.; Zhang, X.; Zhang, W.; Shi, L. *Langmuir* **2006**, *22*(22), 9393–9396.

(53) Duwez, A. S.; Guillet, P.; Colard, C.; Gohy, J. F.; Fustin, C. A. *Macromolecules* **2006**, *39*(8), 2729–2731.

presence of AuNPs. A similar result was also obtained when a block copolymer synthesized in the reverse order, i.e., PNIPAM-*b*-PBA, was used as stabilizer. Besides, the solubilities of the obtained nanohybrids in different solvents (vide infra) corresponds mainly to the one of PNIPAM homopolymer. On the other hand, when NPs were coated with $PNIPAM_{10k}$ the SPB maximum wavelength appeared at higher value ca. 528 nm. Therefore, in the case of homopolymer, the stabilization mechanism strongly differs from the one of diblock polymer. This result was further confirmed by following the changes in the surface plasmon band of AuNPs as a function of temperature. The influence of turbidity of the solution was removed by first subtracting the increase in absorbance at 800 nm, then by normalizing the curves at 400 nm and multiplying by a factor in a way that these absorbances vary from 1 to 0. Indeed, the surface plasmon band of AuNPs was sensitive to many factors including the refractive index in the surroundings of the NPs. The collapse of PNIPAM at LCST due to the dehydratation of the polymer chains usually induced a significant decrease in $I_{max}$ and a slight modification of $\lambda_{max}$.[47a,49a] Effectively, such modifications were observed for Au@PNIPAM hybrids (see the Supporting Information, Figure S7). Whereas this effect was still observed in the case of $Au@PBA_{2k}$-*b*-$PNIPAM_{8k}$, its amplitude decreased significantly as shown in panels A and B in Figure 7. Interestingly, almost no modification was observed in the case of $Au@PBA_{5k}$-*b*-$PNIPAM_{5k}$ (Figure 7B). The change in the surface plasmon band was observed to be reversible as the temperature was lowered back to 25 °C. Such discrepancies may arise from the nature of the polymer in direct interaction with the surface of the NPs. All results tend to demonstrate that the gold core was surrounded by an inner layer mainly made of PBA segments and an outer layer made of PNIPAM. Nevertheless, the precise nature of interaction with the gold surface might rely on a more complex mechanism that has yet to be elucidated.

Another interesting feature arose from the observation by UV−visible spectroscopy of nanohybrids containing high levels of polymer (see the Supporting Information, Figures S8−S10). When increasing amounts of polymer, the solution of nanohybrids based on the homopolymer PNIPAM solution turns to slightly red-purple, whereas copolymer solutions remained unchanged. In UV−visible spectra, this change was linked to an increase of full width at half-maximum intensity of SPB with PNIPAM concentration. As the NPs size remained the same in all experiments, this observation was mainly related to the aggregation state of the NPs in a single nanohybrid.[26a] Indeed, it was observed by TEM measurements (see the Supporting Information, Figure S11) that several NPs were associated inside the same Au@PNIPAM hybrid. Although stability remains the same for all nanohybrids, copolymer structures were demonstrated to be more efficient than the homopolymer at obtaining nanohybrids composed of isolated/noninteracting AuNPs.

The morphology and size of the nanohybrids obtained with $PBA_{2k}$-*b*-$PNIPAM_{8k}$ and $PBA_{5k}$-*b*-$PNIPAM_{5k}$, including the distribution of the particles within the

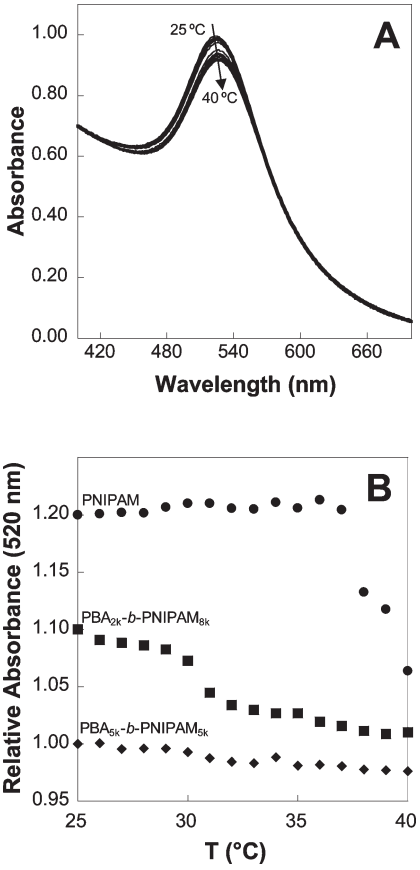


**Figure 7.** (A) Changes in absorption spectra of $Au@PBA_{2k}$-*b*-$PNIPAM_{8k}$ with increasing temperature. The absorbance at 800 nm was subtracted from the spectra, and then normalized at 400 nm to remove scattering contribution and multiplied by a factor in a way that absorbances vary from 0 to 1. [AuNPs] = $2.5 \times 10^{-4}$ mol $L^{-1}$ and [polymer] = 0.01 wt %. (B) Relative absorbance at 520 nm as a function of temperature for $Au@PNIPAM_{10k}$, $Au@PBA_{2k}$-*b*-$PNIPAM_{8k}$ and $Au@PBA_{5k}$-*b*-$PNIPAM_{5k}$. The two first curves were shifted by 0.1 and 0.2 for clarity reasons.

polymer matrix was further investigated by diffusion and microscopy measurements. For comparison purpose, the corresponding PNIPAM homopolymer was also investigated. The hydrodynamic radius in aqueous solutions of the different NP/polymer composites was first studied by DLS. Figure 8 shows the hydrodynamic diameter of $PBA_{2k}$-*b*-$PNIPAM_{8k}$ or $PNIPAM_{10k}$-coated and bare NPs as a function of temperature.

At 25 °C, bare NPs have a hydrodynamic radius around 10 nm. The coating of these NPs with $PNIPAM_{10k}$ increased its value up to 24 nm, far from the one corresponding to $PNIPAM_{10k}$ alone (5.9 nm). Interestingly, AuNPs coated with $PBA_{2k}$-*b*-$PNIPAM_{8k}$ have a hydrodynamic diameter around 30 nm comparable to the one observed for $PBA_{2k}$-*b*-$PNIPAM_{8k}$ aggregates. Similar trends were observed for $PBA_{5k}$-*b*-$PNIPAM_{5k}$-coated NPs. TEM experiments were then performed to better understand those results and to investigate the location of AuNPs within polymer aggregates. Figure 9 displays a typical set of images obtained after negative staining from $Au@PNIPAM_{10k}$, $Au@PBA_{2k}$-*b*-$PNIPAM_{8k}$ or $Au@PBA_{5k}$-*b*-$PNIPAM_{5k}$ dispersions prepared with a polymer concentration of 0.1 wt %. No bare AuNPs were observed. For all systems, the hybrid Au/polymer particles

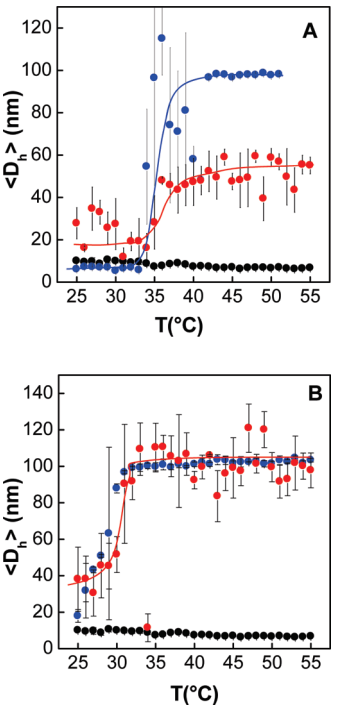


**Figure 8.** Variation in hydrodynamic diameter of (A) AuNPs (black), $PNIPAM_{10k}$ (blue), and $Au@PNIPAM_{10k}$ (red) and (B) AuNPs (black), $PBA_{2k}$-*b*-$PNIPAM_{8k}$ (blue), and $Au@PBA_{2k}$-*b*-$PNIPAM_{8k}$ (red) with temperature. [AuNPs] = $5 \times 10^{-4}$ mol $L^{-1}$ and [polymer] = 0.025 wt %. The lines are guides for the eye.

clearly showed to have a core−shell morphology, the dark cores corresponding to the electron-dense Au atom embedded into a more or less circular brighter polymer shell. The overall sizes of those composites were, respectively, 13 ± 6, 16 ± 4, and 20 ± 9 nm. Although NPs core size remains roughly constant, the shell size increases with larger hydrophobic content. Numerous free polymer globules were also present in the case of copolymer coated NPs, whereas such structures were not seen with $PNIPAM_{10k}$. Indeed, the polymer concentration in the copolymer dispersion was kept above the CAC. The presence of such aggregates could explain results from DLS measurements as they participate to the whole signal, inducing larger dispersity and hindering signal from nanohybrids.

Experimental results obtained above the cloud point temperature showed similar trends. In the case of PNIPAM-coated AuNPs, hydrodynamic radii were significantly different from the one of PNIPAM mesoglobules (50 and 100 nm, respectively), while for $PBA_{2k}$-*b*-$PNIPAM_{8k}$ and $PBA_{5k}$-*b*-$PNIPAM_{5k}$ coated AuNPs, hydrodynamic radii remain the same in the presence of NPs but with larger distribution. Once again, as observed by TEM, the presence in solution of numerous free mesoglobules, in addition to coated AuNPs explains this result.

The data collected by DLS, UV−visible, and TEM experiments all demonstrate that the copolymers were adsorbed on the surface of AuNPs to form nonmicellar aggregates that can be significantly smaller than the size of micelles or mesoglobules. A mechanism involving an equilibrium between polymer forming aggregates and coated around NPs may be involved. This is in good agreement with literature

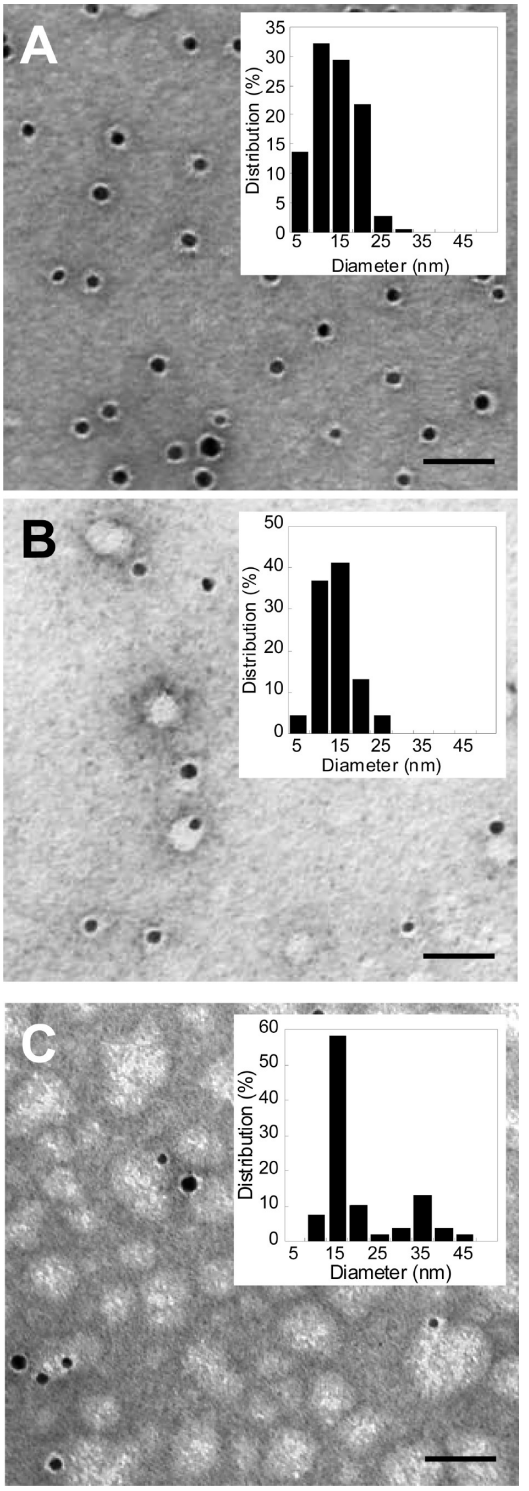


**Figure 9.** TEM images (negative stain) and distribution of (A) $AuNPs@PNIPAM_{10k}$; (B) $AuNPs@PBA_{2k}$-*b*-$PNIPAM_{8k}$ and (C) $AuNPs@PBA_{5k}$-*b*-$PNIPAM_{5k}$ nanohybrids (scale bar = 100 nm). [AuNPs] = $5 \times 10^{-4}$ mol $L^{-1}$ and [polymer] = 0.1 wt %.

results: when the radius of the particle is larger than the radius of gyration of the polymer (8 ± 2 nm and 5 ± 2 nm for AuNPs and $PBA_{2k}$-*b*-$PNIPAM_{8k}$, respectively), the polymer adsorbs upon each individual particle as on a flat surface.[54]

(54) Hershkovits, E.; Tannenbaum, A.; Tannenbaum, R. *J. Phys. Chem. B* **2008**, *112*(17), 5317–5326.

It can be seen in Figure 7B, that the cloud point temperature of the thermoresponsive copolymers were not modified by the presence of AuNPs (29.9 °C vs 30.0 °C for Au@$PBA_{2k}$-*b*-$PNIPAM_{8k}$). However, in previous works on Au@PNIPAM nanohybrids, when a linkage between NPs and PNIPAM was created by the "grafting to" or the "grafting from" methods, a change in the transition temperature was observed.[48g] Indeed, when a polymer bound to a NP undergoes a transition from an extended hydrophilic chain to a globular hydrophobic structure, it will collapse in only one direction, that is, toward the NP. Moreover, a NP effectively confines a cluster of thermosensitive polymer chains within a limited space, favoring the hydrophilic to hydrophobic transition. Hence, a decrease of cloud temperature from 33.5 to 28.4 °C was observed for nanohybrids with a PNIPAM shell ($M_n$ = 4600 g $mol^{-1}$) attached by a thiol to the gold surface, whereas no effect was observed with polymer bearing no thiol terminal group.[48g] It was also observed that by decreasing the molar mass of brush chain from ca. 3300 to 700 g $mol^{-1}$, the phase transition temperature shifted from 31 to 15 °C for nanohybrids, whereas this temperature increase for free polymer chain shows in solution.[49d] In our case, the absence of such effect could be explained in part by the relative "high" $M_n$ value of the PNIPAM sample (10 000 g $mol^{-1}$) and by the weak interactions of polymer chains with the surface of AuNPs (comparatively to the one obtained by the "grafting from" approach).

Maintaining the AuNPs solution above $T_c$ for several hours results in the formation of a red precipitate that could be redispersed rapidly by cooling the solution below $T_c$. UV−visible measurements showed no change in their spectroscopic properties after several heating−cooling cycles (see the Supporting Information, Figure S13) and so confirmed the complete reversible nature of the transition at $T_c$.

Hence, TEM images obtained from sample above $T_c$ showed small aggregates of particles with corona that does not differ significantly from the one observed below $T_c$ in addition to some particle inside or in interaction with mesoglobules (see the Supporting Information, Figure S8 and Figure 3).

*3.3.2. In situ Formation of AuNPs.* An additional control over size and shape of inorganic core could be obtained by addition of the polymer during the growing stage of AuNPs as described for other systems.[55] Thus, in situ formation of AuNPs below and above $T_c$ was then investigated by carrying out the reduction by $NaBH_4$ of the $HAuCl_4$ sol in the presence of $PBA_{2k}$-*b*-$PNIPAM_{8k}$ at block copolymer concentrations ranging from $6.5 \times 10^{-4}$ to $1.5 \times 10^{-1}$ wt %.

First, we studied the effect of polymer concentration on the kinetics of AuNPs formation at room temperature. The reduction was slower when the amount of polymer added was higher, as could be observed by the rate of increase of the optical density at 520 nm (Figure 10A). Besides, the final solution color (related to the SPB wavelength) varied from dark brown to light orange depending on the polymer concentration (see the Supporting Information, Figure S12). TEM images of the so-obtained Au@$PBA_{2k}$-*b*-$PNIPAM_{8k}$ NPs showed that the concentration of block copolymer had a strong influence on the final size and polydispersity of particles (Figure 10B). Indeed, in the absence of polymer, the mean size of particles was 6 ± 3 nm. For a low polymer concentration (typically $2.5 \times 10^{-3}$ wt %), it was found around 8 ± 6 nm, corresponding to highly polydisperse particles, whereas for a high polymer concentration (like 1.5 wt %), the mean diameter dramatically decreased to 1.6 ± 0.4 nm. This could be correlated to the kinetic effect previously described: the slower the kinetics of reduction, the more nuclei can be formed, leading to an increasing number of smaller particles with a better control of polydispersity. Therefore, the in situ formation appears as a very straightforward way to control the size of Au@$PBA_{2k}$-*b*-$PNIPAM_{8k}$ NPs by simply adjusting the initial polymer concentration as already observed for other polymeric systems.[55b,56] For the experiments carried out above $T_c$, at 45 °C, similar results were obtained, leading to the formation of nanohybrids with a quite similar size control.

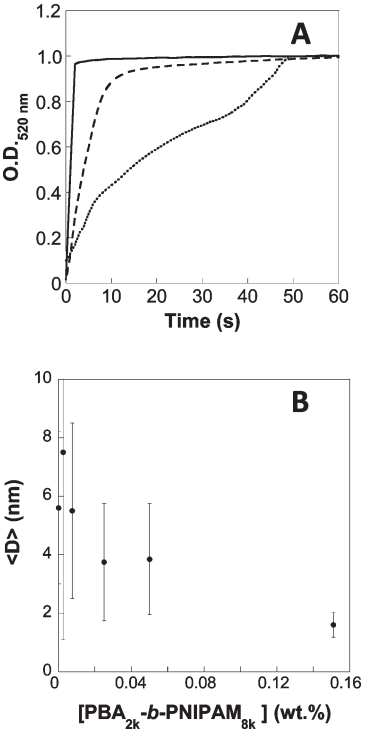


**Figure 10.** (A) Kinetics of appearance of SPB (followed at 520 nm) for a $PBA_{2k}$-*b*-$PNIPAM_{8k}$ concentration of $1 \times 10^{-3}$ wt % (solid line), $1 \times 10^{-2}$ wt % (dashed line) and $1 \times 10^{-1}$ wt % (dotted line). The absorbance values were normalized by dividing by the corresponding absorbance at 60 s. (B) Effect of the initial polymer concentration on the mean diameter of NPs (determined by TEM measurements).

(55) (a) Kramer, M.; Perignon, N.; Haag, R.; Marty, J. D.; Thomann, R.; Lauth-de Viguerie, N.; Mingotaud, C. *Macromolecules* **2005**, *38* (20), 8308–8315. (b) Perignon, N.; Marty, J. D.; Mingotaud, A. F.; Dumont, M.; Rico-Lattes, I.; Mingotaud, C. *Macromolecules* **2007**, *40* (9), 3034–3041.

(56) Marty, J. D.; Martinez-Aripe, E.; Mingotaud, A. F.; Mingotaud, C. *J. Colloid Interface Sci.* **2008**, *326*(1), 51–54.

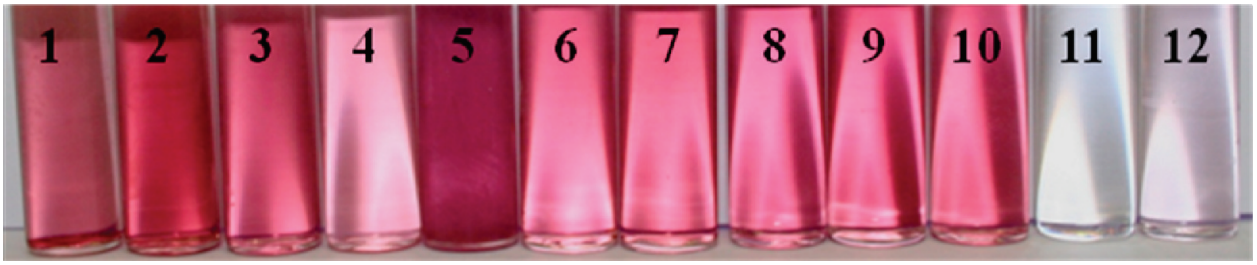


**Figure 11.** Redispersion of dried AuNPs@$PBA_{2k}$-*b*-$PNIPAM_{8k}$ nanohybrids in different solvents: **1**, water; **2**, methanol; **3**, ethanol; **4**, acetonitrile; **5**, DMSO; **6**, DMF; **7**, acetone; **8**, dichloromethane; **9**, chloroform; **10**, THF; **11**, toluene; **12**, cyclohexane.

On the other hand, the maxima of the surface plasmon band of the nanohybrids prepared in situ at polymer concentrations lower than 0.05 wt % appeared at longer wavelengths than those obtained by coating of preformed AuNPs. This suggests that probably another mechanism of stabilization is involved.

*3.3.3. Stabilization Properties.* The initial bare hydrophilic AuNPs were poorly stable over time when increasing initial ionic strength or changing initial pH value (i.e., 8) conditions. As already mentioned, the coating of bare AuNPs with $PBA_{2k}$-*b*-$PNIPAM_{8k}$ and $PBA_{5k}$-*b*-$PNIPAM_{5k}$ dramatically increased their stability: no evolution of the UV spectra was observed for a wide range of pH values (1−13) (see the Supporting Information, Figure S12) and for increasing ionic strength up to 1 mol $L^{-1}$. Moreover, after drying, the resulting red powder could be easily redispersed in a wide range of concentrations (up to 1 wt %) and polar or chlorinated solvents (water, methanol, ethanol, acetonitrile, DMSO, DMF, dichloromethane, chloroform, and THF). However, as expected, they could not be redispersed in apolar solvents such as toluene and cyclohexane (Figure 11). Slight differences in color were attributed to the change of the refractive index of the surrounding medium, which has influence on the position of the SPB (shift to red from 2 to 6 nm for the DMSO). Similar results were obtained for the nanohybrids obtained by in situ formation.

## 4. Conclusions

PNIPAM-based amphiphilic block copolymers were prepared with different hydrophobic content using the MADIX/RAFT process, and their properties were studied in aqueous solutions at different temperatures. At 20 °C, both $PBA_{2k}$-*b*-$PNIPAM_{8k}$ and $PBA_{5k}$-*b*-$PNIPAM_{5k}$ block copolymers self-assembled forming spherical micelles with a diameter of, respectively, ca. 28 and 60 nm, as evidenced by DLS, SANS, and TEM. When these aqueous solutions were heated, a cloud point was observed that was lower for the block copolymer with the longer PBA block (28.1 °C vs. 29.9 °C). Besides, instead of forming irregular large aggregates upon temperature increase, mesoglobules with defined sizes appeared in both cases. These polymers were then employed as stabilizers of AuNPs dispersions by either a posteriori adsorption on AuNPs or in situ formation. Both approaches were successful for stabilization and reversibility of the thermostimulable precipitation process was demonstrated. Moreover, we showed that in the first method, the stabilization mechanism was neither based on the adsorption of micelles nor on the chemisorption of the xanthate group. Instead, it is probable that the polymer aggregates play the role of a reservoir of polymer chains, which adsorb individually onto the NP. In the second method, it was observed that the size of Au nanohybrids could be tuned by the amount of polymer that was added. In both cases, stable NPs in a wide range of solvents and ionic strength were obtained. This strategy should be easily applied to other type of metal NPs, and should lead to useful "smart" materials for a range of applications including drug delivery and catalysis.[48h]

**Acknowledgment.** The authors thank B. Payré and D. Goudounèche for TEM measurements and Aymeric Guinaudeau for determination of NIPAM transfer constant to Rhodixan A1.

**Supporting Information Available:** Complementary data concerning the behavior in aqueous solution of block copolymers, the stabilization properties of Au@PNIPAM-*b*-PBA nanohybrids, and in situ formation of AuNPs (PDF). This material is available free of charge via the Internet at http://pubs.acs.org.